

## Thermodynamic consistent phase field model for sintering process with multiphase powders

Rui-jie ZHANG<sup>1</sup>, Zhong-wei CHEN<sup>2</sup>, Wei FANG<sup>1</sup>, Xuan-hui QU<sup>1,3</sup>

1. Institute for Advanced Materials Technology, University of Science and Technology Beijing, Beijing 100083, China;

2. State Key Laboratory of Solidification Processing, Northwestern Polytechnical University, Xi'an 710072, China;

3. State Key Laboratory for Advanced Metals and Materials, University of Science and Technology Beijing, Beijing 100083, China

Received 24 April 2013; accepted 9 August 2013

**Abstract:** A thermodynamic consistent phase field model is developed to describe the sintering process with multiphase powders. In this model, the interface region is assumed to be a mixture of different phases with the same chemical potential, but with different compositions. The interface diffusion and boundary diffusion are also considered in the model. As an example, the model is applied to the sintering process with Fe–Cu powders. The free energy of each phase is described by the well-developed thermodynamic models, together with the published optimized parameters. The microstructure and solute distribution during the sintering process can both be obtained quantitatively.

**Key words:** phase field model; sintering; multiphase powder; thermodynamics

### 1 Introduction

Sintering is an effective method to create parts from powders, specifically for those with high melting temperature and hard to generate by casting method [1]. In most sintering processes the powdered material is heated to a temperature below the melting point. The atoms in the powder particles diffuse across the particles boundaries, fusing the particles together and creating one solid body.

Recently, the phase-field model is becoming a powerful tool which can describe the complex interface pattern evolutions [2]. It describes the microstructure using a set of conserved and non-conserved field variables that are continuous across the interface regions. Phase-field models have been widely used in solidification [3–5], precipitation [6–8], grain growth [9–11] and dislocation movement [12,13] area.

Phase field models for sintering process were already developed by WANG and LIU [14,15], WANG [16] and KUMAK and FANG [17] based on the system density field. Recently, ASP and ÅGREN [18] set up a

thermodynamic consistent phase field model for sintering process based on the vacancy diffusion approach. But all of them were only for powders with pure substance.

Sintering with multiphase powders is widely adopted in industry, such as Fe–Ni system, Fe–Cu system and Cu–Al system. It is not convenient to describe the particle growth and solute diffusion in multiphase powders with the previous pure substance models. In this work, we develop a thermodynamic consistent phase field model for multiphase powders sintering process. In the model, every point is assumed to be a mixture of different phases with the same chemical potential, but with different compositions. Boundary diffusion and surface diffusion are also considered in the model. As an example, we apply this model to the sintering process with Fe–Cu powders.

### 2 Phase field model

#### 2.1 Governing equations

In this work, the free energy density is defined as follows [19]:

**Foundation item:** Project (2011CB606306) supported by the National Basic Research Program of China; Project (51101014) supported by the National Natural Science Foundation of China; Project (SKLSP201214) supported by the State Key Laboratory of Solidification Processing in Northwestern Polytechnical University, China

**Corresponding author:** Xuan-hui QU; Tel: +86-10-62332700; E-mail: [quxh@ustb.edu.cn](mailto:quxh@ustb.edu.cn)  
DOI: 10.1016/S1003-6326(14)63126-5

$$f = \sum_{i=1}^N h(\phi_i) f_i(C_{i,1}, \dots, C_{i,M-1}) + \sum_{i=1}^N \sum_{j>i}^N w_{i,j} \phi_i \phi_j \quad (1)$$

where  $N$  is the total number of particles;  $M$  is the total number of substances, which includes vacancy;  $f_i(C_{i,1}, \dots, C_{i,M-1})$  is the free energy density of phase  $i$  with compositions  $(C_{i,1}, \dots, C_{i,M-1})$ ;  $w_{i,j}$  is the height of the double well potential; the parabolic double well potential  $\phi_i \phi_j$  is defined in the interfacial region only where  $0 < \phi_i < 1$  and  $0 < \phi_j < 1$ ;  $h(\phi)$  is the interpolation function which satisfies  $h(0)=0$  and  $h(1)=1$ .

In order to make sure  $\sum_{i=1}^N h(\phi_i) = 1$ , we simply use  $h(\phi) = \phi$  in this work.

The total free energy of the system is defined as follows:

$$F = \int_V \left[ \sum_{i=1}^N \sum_{j>i}^N \left( -\frac{\varepsilon_{ij}^2}{2} \nabla \phi_i \nabla \phi_j + w_{i,j} \phi_i \phi_j \right) + \sum_{i=1}^N \phi_i f_i(C_{i,1}, \dots, C_{i,M-1}) \right] dV \quad (2)$$

where  $\varepsilon_{ij}$  is the gradient energy coefficient. At each point, the compositions of different phases are not independent and constrained by the following conditions:

$$\frac{\partial f_1}{\partial C_{1,p}} = \frac{\partial f_2}{\partial C_{2,p}} = \dots = \frac{\partial f_N}{\partial C_{N,p}} = \mu_p, p=1, 2, \dots, M-1 \quad (3)$$

The solute composition at a given point can be described as follows:

$$C_p = \sum_{i=1}^N \phi_i C_{i,p}, p=1, 2, \dots, M-1 \quad (4)$$

The sum of each phase field parameter at any location in the system is conserved:

$$\sum_{i=1}^N \phi_i = 1 \quad (5)$$

The governing equations for phase field and solute composition can then be written as

$$\frac{\partial \phi_i}{\partial t} = -\sum_{j \neq i}^N L_{ij} \left( \frac{\delta F}{\delta \phi_i} - \frac{\delta F}{\delta \phi_j} \right) \quad (6)$$

$$\frac{\partial C_p}{\partial t} = \nabla \sum_{q=1}^{M-1} M_{pq} \nabla \frac{\delta F}{\delta C_q} \quad (7)$$

where  $L_{ij}$  is phase field mobility and  $M_{pq}$  is solute diffusion mobility.

The variation term in Eq.(6) and Eq.(7) can be given as

$$\begin{aligned} \frac{\delta F}{\delta \phi_i} &= \sum_{j \neq i}^N \left( \frac{\varepsilon_{ij}^2}{2} \nabla^2 \phi_j + w_{i,j} \phi_j \right) + \\ &\left( f_i + \sum_{k=1}^N \phi_k \sum_{p=1}^{M-1} \frac{\partial f_k}{\partial C_{k,p}} \frac{\partial C_{k,p}}{\partial \phi_i} \right) = \\ &\sum_{j \neq i}^N \left( \frac{\varepsilon_{ij}^2}{2} \nabla^2 \phi_j + w_{i,j} \phi_j \right) + \\ &\left( f_i + \sum_{p=1}^{M-1} \mu_p \sum_{k=1}^N \phi_k \frac{\partial C_{k,p}}{\partial \phi_i} \right) \end{aligned} \quad (8)$$

$$\frac{\delta F}{\delta C_q} = \sum_{k=1}^N \phi_k \sum_{p=1}^{M-1} \frac{\partial f_k}{\partial C_{k,p}} \frac{\partial C_{k,p}}{\partial C_q} = \sum_{p=1}^{M-1} \mu_p \sum_{k=1}^N \phi_k \frac{\partial C_{k,p}}{\partial C_q} \quad (9)$$

If we do the partial difference on Eq. (4) with respect to  $\phi_i$  and  $C_p$ , respectively, we will get

$$C_{i,p} + \sum_{k=1}^N \phi_k \frac{\partial C_{k,p}}{\partial \phi_i} = 0 \quad (10)$$

$$\sum_{k=1}^N \phi_k \frac{\partial C_{k,p}}{\partial C_q} = \delta_{pq} \quad (11)$$

where  $\delta_{pq}$  is the Kronecker delta and it is 1 when  $p = q$  and 0 when  $p \neq q$ .

Inputting Eq. (10) and Eq. (11) into Eq. (8) and Eq. (9), we can get

$$\frac{\delta F}{\delta \phi_i} = \sum_{j \neq i}^N \left( \frac{\varepsilon_{ij}^2}{2} \nabla^2 \phi_j + w_{i,j} \phi_j \right) + \left( f_i - \sum_{p=1}^{M-1} \mu_p C_{i,p} \right) \quad (12)$$

$$\frac{\partial C_p}{\partial t} = \nabla \sum_{q=1}^{M-1} M_{pq} \nabla \frac{\delta F}{\delta C_q} = \nabla \sum_{q=1}^{M-1} M_{pq} \nabla \mu_q \quad (13)$$

## 2.2 Surface and grain boundary diffusion

If we assume the diffusion mobility  $M_{pq}$  has the following form:

$$M_{pq} = \sum_{k=1}^N [\phi_k M_{pq}^{\text{BK},k} + (\xi |\nabla \phi_k|) M_{pq}^{\text{BY},k}] \quad (14)$$

where  $M_{pq}^{\text{BK},k}$  is the bulk diffusion mobility;  $M_{pq}^{\text{BY},k}$  is the boundary diffusion mobility; BY and BK in the superscript mean the bulk and boundary, respectively;  $\xi$  is a scaling factor and can be given as  $2\lambda$ , where  $2\lambda$  is the interface thickness. We know that  $|\nabla \phi_k|$  is about  $1/(2\lambda)$  in the interface area and approaches to 0 in the bulk phase area. By multiplying with  $\xi$ ,  $\xi |\nabla \phi_k|$  will approach to 1 at the interface and 0 in the bulk phase, respectively.

Inserting Eq. (14) into Eq. (13), we will get

$$\frac{\partial C_p}{\partial t} = \nabla \sum_{q=1}^{M-1} \left\{ \sum_{k=1}^N [\phi_k M_{pq}^{\text{BK},k} + (\xi |\nabla \phi_k|) M_{pq}^{\text{BY},k}] \right\} \nabla \mu_q \quad (15)$$

According to Eq. (3), we can re-write Eq. (15) as

$$\frac{\partial C_p}{\partial t} = \nabla \sum_{q=1}^{M-1} \left\{ \sum_{k=1}^N [\phi_k M_{pq}^{BK,k} + (\xi |\nabla \phi_k|) M_{pq}^{BY,k}] \cdot \sum_{r=1}^{M-1} \frac{\partial^2 f_k}{\partial C_{k,q} \partial C_{k,r}} \nabla C_{k,r} \right\} = \nabla \left( \sum_{k=1}^N \phi_k \sum_{q=1}^{M-1} M_{pq}^{BK,k} \sum_{r=1}^{M-1} f_{qr}^k \nabla C_{k,r} + \sum_{k=1}^N \xi |\nabla \phi_k| \sum_{q=1}^{M-1} M_{pq}^{BY,k} \sum_{r=1}^{M-1} f_{qr}^k \nabla C_{k,r} \right) \quad (16)$$

where  $f_{qr}^k = \frac{\partial^2 f_k}{\partial C_{k,q} \partial C_{k,r}}$ . If we put

$$\sum_{q=1}^{M-1} M_{pq}^{BK,k} f_{qr}^k = D_{pr}^{BK,k} \quad (17)$$

$$\sum_{q=1}^{M-1} M_{pq}^{BY,k} f_{qr}^k = D_{pr}^{BY,k} \quad (18)$$

Eq. (16) can be re-written as

$$\frac{\partial C_p}{\partial t} = \nabla \left( \sum_{k=1}^N \phi_k \sum_{r=1}^{M-1} D_{pr}^{BK,k} \nabla C_{k,r} + \sum_{k=1}^N \xi |\nabla \phi_k| \sum_{r=1}^{M-1} D_{pr}^{BY,k} \nabla C_{k,r} \right) \quad (19)$$

where  $D_{pr}^{BK,k}$  is the bulk diffusion coefficient in phase  $k$  and  $D_{pr}^{BY,k}$  is the boundary diffusion coefficient for phase  $k$ . If we consider the bulk diffusion coefficients matrix  $D^{BK,k}$ ,  $D_{pr}^{BK,k}$  will be the diagonal components of  $D^{BK,k}$  when  $p = r$  and the off-diagonal components when  $p \neq r$ . It is the same thing for boundary diffusion coefficients matrix  $D^{BY,k}$ . If we assume that  $N$  is the gas phase,  $D_{pr}^{BY,N}$  will be the surface diffusion coefficient.

### 2.3 Parameters in phase field equation

In order to find the relationship between materials properties and parameters in phase field model, a one-dimensional problem at the equilibrium state is considered. If we only consider the phase transformation between two phases,  $\phi_i$  and  $\phi_j$ , the one-dimensional phase field profile can be obtained [19]:

$$\phi_i = \frac{1}{2} \left( 1 - \sin \frac{\sqrt{2w_{ij}}}{\varepsilon_{ij}} x \right) \quad (20)$$

Then, the following relationships can be obtained:

$$2\lambda = \pi \frac{\varepsilon_{ij}}{\sqrt{2w_{ij}}} \quad (21)$$

$$\sigma_{ij} = \frac{\pi}{8} \varepsilon_{ij} \sqrt{2w_{ij}} \quad (22)$$

### 2.4 Thermodynamic descriptions of system

In multicomponent alloys, the integral Gibbs energy for each phase depends on its constitution, temperature and pressure, and this can be described by a thermodynamic model [20]:

$$G = G_0 + G_{mix}^{ideal} + G_{ex} \quad (23)$$

where  $G_0$  is the contribution of the pure components to the Gibbs free energy,  $G_{mix}^{ideal}$  is the ideal mixing contribution and  $G_{ex}$  is the Gibbs excess energy which is caused by the non-ideal interaction between the components.

There are a large number of thermodynamic models for various substances in different states, such as the Redlich–Kister–Muggianu formalism [21] for face-centered cubic, body-centered cubic and hexagonal close packed solid solution phases and the sublattice model [22] for the description of a phase with two or more sublattices. In order to quantitatively describe the thermodynamics of the system, a lot of thermodynamic databases [23] have also been set up together with those thermodynamic models.

## 3 Application to sintering process with Fe and Cu powders

### 3.1 Thermodynamic description for Fe–Cu–H system

For Fe-based sintered parts, Cu is an effective solid solution strengthening element. Fe–Cu powders are usually sintered at about 1000 °C and protected by H<sub>2</sub> reducing atmosphere. At this temperature, both Fe and Cu particles have FCC structures. So for Fe and Cu particles, they both can be described by a same sublattice model [24], i.e., (Fe,Cu)<sub>1</sub>(H,Va)<sub>1</sub>, where Va means vacancy. The Gibbs free energy of the FCC phase can then be given as

$$G^{FCC} = y_{Fe} (y_{Va} G_{Fe:Va}^{FCC} + y_H G_{Fe:H}^{FCC}) + y_{Cu} (y_{Va} G_{Cu:Va}^{FCC} + y_H G_{Cu:H}^{FCC}) + G_{id}^{FCC} + G_{ex}^{FCC} \quad (24)$$

$$G_{id}^{FCC} = RT \sum_i y_i \ln y_i, \quad i = Fe, Cu, H, Va \quad (25)$$

$$G_{ex}^{FCC} = y_{Fe} y_{Cu} \left[ y_{Va} \sum_{v=0}^n L_{Fe,Cu:Va}^{FCC} (y_{Fe} - y_{Cu})^v + y_H \sum_{v=0}^n L_{Fe,Cu:H}^{FCC} (y_{Fe} - y_{Cu})^v \right] + y_H y_{Va} \left[ y_{Fe} \sum_{v=0}^n L_{Fe:H,Va}^{FCC} (y_H - y_{Va})^v + y_{Cu} \sum_{v=0}^n L_{Cu:H,Va}^{FCC} (y_H - y_{Va})^v \right] \quad (26)$$

where  $y_i$  is the site fraction of component  $i$  in its sublattice. For the gas phase, we assume that it consists

of H, H<sub>2</sub>, Fe and Cu and all the species mix ideally. Its Gibbs energy can be given as

$$G^{\text{gas}} = \sum_i C_i G_{i,0}^{\text{gas}} + RT \sum_i C_i \ln x_i + RT \ln(P/P_0) \quad (27)$$

where  $C_i$  is the mole fraction of the  $i$ th species in the gas phase;  $G_{i,0}^{\text{gas}}$  is the standard Gibbs energy of the  $i$ th species;  $P_0$  is the standard pressure.

The thermodynamics parameters for both FCC and gas phase in Fe–Cu–H system can be found in Refs. [25–27]. The other parameters used in the simulation are shown in Table 1. The phase field mobility  $L_{ij}$  in Eq. (6) is related to the interface kinetics [28], and a constant value of 0.001 is adopted [29] for all the phases in this work.

**Table 1** Parameters used in simulation for Fe–Cu system

Parameter	Value
Surface energy between Fe particle and gas	2.6 J/m <sup>2</sup> [30]
Surface energy between Cu particle and gas	1.6 J/m <sup>2</sup> [30]
Interface energy between Fe particle and Cu particle	0.3 J/m <sup>2</sup> [31]
Self diffusion coefficient of Fe	4.06×10 <sup>-8</sup> m <sup>2</sup> /s [32]
Self diffusion coefficient of Cu	5.45×10 <sup>-7</sup> m <sup>2</sup> /s [33]
Bulk diffusion coefficient of Fe in Cu	4.59×10 <sup>-7</sup> m <sup>2</sup> /s [34]
Bulk diffusion coefficient of H in Cu	2.87×10 <sup>-6</sup> m <sup>2</sup> /s [35]
Bulk diffusion coefficient of Cu in Fe	4.05×10 <sup>-8</sup> m <sup>2</sup> /s [36]
Bulk diffusion coefficient of H in Fe	1.64×10 <sup>-8</sup> m <sup>2</sup> /s [35]
Boundary and surface diffusion coefficient of Fe	4.25×10 <sup>-6</sup> m <sup>2</sup> /s [37]
Boundary and surface diffusion coefficient of Cu	7.83×10 <sup>-8</sup> m <sup>2</sup> /s [38]
Sintering temperature	1000 °C
Grid size	10 nm

### 3.2 Numerical treatment

The governing equations for phase field (Eq. 6) and concentration (Eq. 19) evolution were solved by finite difference method. In this work, we only consider Fe, Cu and H species. There are six independent concentrations to be determined in Eq. (4). They are  $C_{1,\text{Cu}}$ ,  $C_{2,\text{Cu}}$ ,  $C_{3,\text{Cu}}$ ,  $C_{1,\text{Fe}}$ ,  $C_{2,\text{Fe}}$  and  $C_{3,\text{Fe}}$ , where the subscript 1 means the FCC Fe phase, 2 means the FCC Cu phase and 3 means gas phase. For each species, the concentration equilibrium (Eq. (3)) between different phases must be achieved anytime at each grid. Input the Gibbs energy for FCC (Eq. 24) and gas (Eq. 27) phase into Eq. (3),  $C_{1,\text{Cu}}$ ,  $C_{2,\text{Cu}}$ ,  $C_{3,\text{Cu}}$ ,  $C_{1,\text{Fe}}$ ,  $C_{2,\text{Fe}}$  and  $C_{3,\text{Fe}}$  can be achieved by solving Eq. (3) together with the concentration conservation equations Eq. (4). This work can be

finished by calling IMSL subroutines in Visual Fortran 6.5 programs.

But only with IMSL subroutines, the solutions of Eqs. (3) and (4) are not stable at every grid. Sometimes we can get minus values for  $C_{1,\text{Cu}}$ ,  $C_{2,\text{Cu}}$ ,  $C_{3,\text{Cu}}$ ,  $C_{1,\text{Fe}}$ ,  $C_{2,\text{Fe}}$  and  $C_{3,\text{Fe}}$ . When this happens, we will not solve Eq. (4) first at those grids. But only with Eq. (3), there are still two independent concentrations left. If we set  $C_{1,\text{Cu}}$  and  $C_{1,\text{Fe}}$  as known parameters, the other four concentrations,  $C_{2,\text{Cu}}$ ,  $C_{3,\text{Cu}}$ ,  $C_{2,\text{Fe}}$  and  $C_{3,\text{Fe}}$ , can be determined. We will set up a database first to store all the equilibrium concentration data as a function of  $C_{1,\text{Cu}}$  and  $C_{1,\text{Fe}}$ .  $C_{1,\text{Cu}}$  changes from 0 to 1 and  $C_{1,\text{Fe}}$  changes from 0 to  $1-C_{1,\text{Cu}}$ , both with a increasing step of 0.0001. This database was constructed using the commercial software Thermo-Calc together with the corresponding thermodynamics descriptions, Eqs. (24) and (27).

Using the above phase equilibrium database, we will find the data array to minimize the following objective function:

$$\text{Sum} = \left[ \left( \sum_{i=1}^3 \phi_i C_{i,\text{Cu}} \right) - C_{\text{Cu}} \right]^2 + \left[ \left( \sum_{i=1}^3 \phi_i C_{i,\text{Fe}} \right) - C_{\text{Fe}} \right]^2 \quad (28)$$

Once the minimum value of sum is achieved, the six concentrations,  $C_{1,\text{Cu}}$ ,  $C_{2,\text{Cu}}$ ,  $C_{3,\text{Cu}}$ ,  $C_{1,\text{Fe}}$ ,  $C_{2,\text{Fe}}$  and  $C_{3,\text{Fe}}$ , will be obtained and can be used for the followed calculations.

### 3.3 Simulation results

Figure 1 shows the microstructure evolution during the sintering process of Fe–Cu particles at different time step. In the real industry, Fe particles are usually mixed with finer Cu particles first. After that, Cu particles will adhere to the surface of Fe particles. This “mixture” will be used as raw materials for the following compaction step. So at the beginning of the simulation, Fe particles are set to be surrounded by finer Cu particles randomly, which is shown in Fig. 1(a). As a strengthening element for Fe-based sintered parts, Cu will dissolve into Fe particles first. Figure 1(b) shows the dissolve process of Cu into Fe particles. We can also see the evolution of sintering neck between Cu and Fe powders in Fig. 1(b). Figure 1(c) shows the end of full dissolution for Cu particles into Fe particles. Figure 1(d) shows the sintering neck growth between Fe particles.

Figure 2 shows the evolution of Cu concentration field during the sintering process. From Figs. 2(a) to (c), we can see that the substance Cu dissolves into Fe particles step by step. Finally, the Cu will distribute uniformly within the Fe particles, which can be seen in Fig. 2(d). It is impossible to describe this phenomenon with the previous pure substance models.

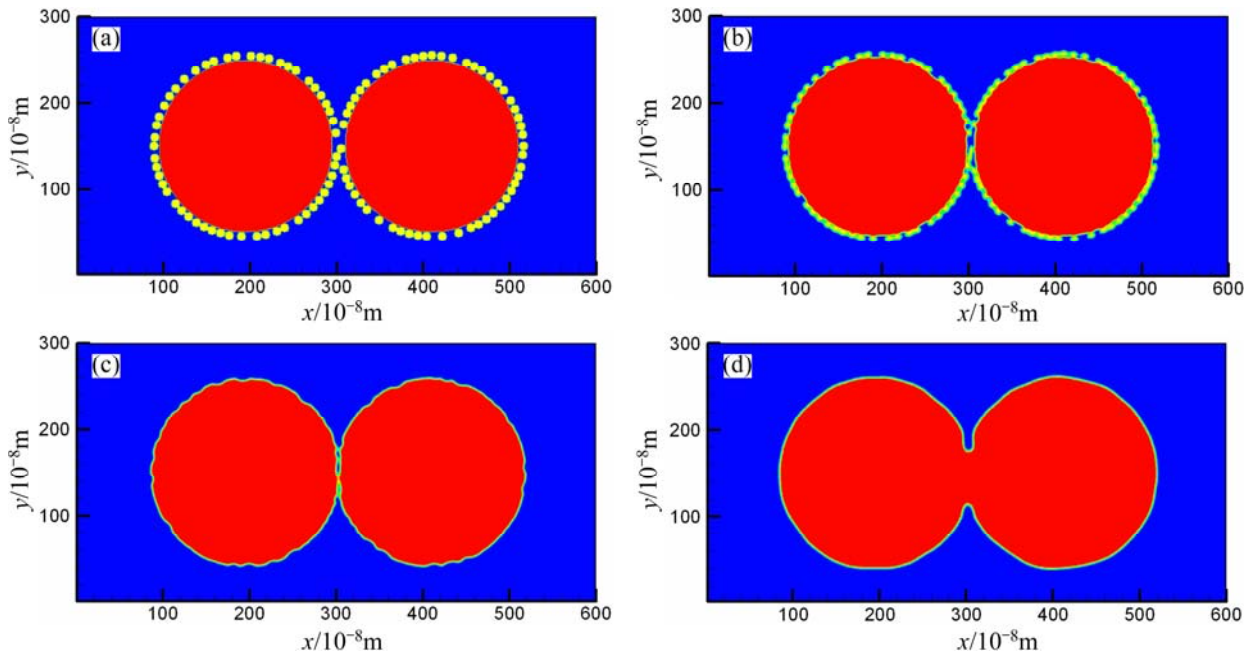


Fig. 1 Microstructure evolution of Fe–Cu powders sintered at 1000 °C: (a)  $t=0$ ; (b)  $t=6\times 10^{-5}$  s; (c)  $t=2.7\times 10^{-4}$  s; (d)  $t=1.8\times 10^{-3}$  s

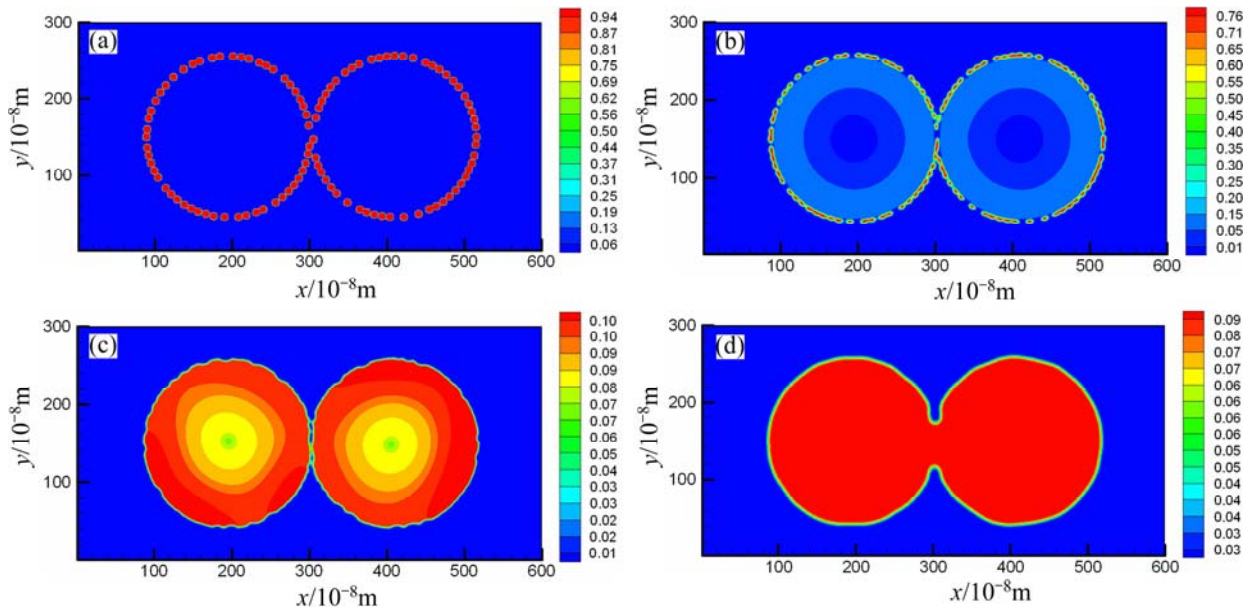


Fig. 2 Concentration field of Cu at different sintering time: (a)  $t=0$ ; (b)  $t=6\times 10^{-5}$  s; (c)  $t=2.7\times 10^{-4}$  s; (d)  $t=1.8\times 10^{-3}$  s

## 4 Conclusions

Powder metallurgy parts with multiphase powders are widely adopted in industry in order to obtain the particular properties. In order to study the sintering process of multiphase powders, we set up a thermodynamic consistent phase field for multiphase system based on the KIM's model. The interface diffusion and boundary diffusion are also considered in the model by using a mixed numerical functions. The free energy of each phase is described by the

well-developed thermodynamic models, together with the published optimized parameters. Since Cu is an effective solid solution strengthening element for Fe based sintered parts, we applied the model to studying the sintering process with Fe–Cu powders. The microstructure and solute distribution during the sintering process can both be obtained quantitatively.

## References

- [1] WAKAI F, BRAKKE K A. Mechanics of sintering for coupled grain boundary and surface diffusion [J]. Acta Materialia, 2011, 59(14):

- 5379–5387.
- [2] CHEN L Q. Phase field models for microstructure evolution [J]. *Annual Review of Materials Research*, 2002, 32(1): 113–140.
- [3] MCFADDEN G B, WHEELER A A, BRAUN R J, CORIELL S R, SEKERKA R F. Phase-field models for anisotropic interfaces [J]. *Physical Review E*, 1993, 48(3): 2016–2024.
- [4] ZHU Chang-sheng, XIAO Rong-zhen, WANG Zhi-ping, FENG Li. Numerical simulation of recalescence of 3-dimensional isothermal solidification for binary alloy using phase-field approach [J]. *Transactions of Nonferrous Metals Society of China*, 2009, 19(5): 1286–1293.
- [5] LONG Wen-yuan, CAI Qi-zhou, CHEN Li-liang, WEI Bo-kang. Phase-field simulations of solidification of Al–Cu binary alloys [J]. *Transactions of Nonferrous Metals Society of China*, 2004, 14(2): 291–296.
- [6] VAITHYANATHAN V, WOLVERTON C, CHEN L Q. Multiscale modeling of  $\theta'$  precipitation in Al–Cu binary alloys [J]. *Acta Materialia*, 2004, 52(10): 2973–2987.
- [7] YANG Kun, CHEN Zheng, WANG Yong-xin, FAN Xiao-li. Microscopic phase-field study on directional coarsening mechanism caused by interaction between precipitates in Ni–Al–V alloy [J]. *Transactions of Nonferrous Metals Society of China*, 2013, 23(1): 193–200.
- [8] AMIROUCHE L, PLAPP M. Phase-field modeling of the discontinuous precipitation reaction [J]. *Acta Materialia*, 2009, 57(1): 237–247.
- [9] CHEN L Q, YANG W. Computer simulation of the domain dynamics of a quenched system with a large number of nonconserved order parameters: The grain-growth kinetics [J]. *Physical Review B*, 1994, 50(21): 15752–15756.
- [10] KRILL III C E, CHEN L Q. Computer simulation of 3-D grain growth using a phase-field model [J]. *Acta Materialia*, 2002, 50(12): 3057–3073.
- [11] FAN D, CHEN L Q. Computer simulation of grain growth using a continuum field model [J]. *Acta Materialia*, 1997, 45(2): 611–622.
- [12] SHEN C, WANG Y. Phase field model of dislocation networks [J]. *Acta Materialia*, 2003, 51(9): 2595–2610.
- [13] WANG Y, LI J. Phase field modeling of defects and deformation [J]. *Acta Materialia*, 2010, 58(4): 1212–1235.
- [14] WANG Y Z, LIU Y H. Simulating microstructural evolution and electrical transport in ceramic gas sensors [J]. *Journal of the American Ceramic Society*, 2000, 83(9): 2219–2226.
- [15] KAZARYAN A, WANG Y Z, PATTON B R. Generalized phase field approach for computer simulation of sintering: Incorporation of rigid-body motion [J]. *Scripta Materialia*, 1999, 41(5): 487–492.
- [16] WANG Y U. Computer modeling and simulation of solid-state sintering: A phase field approach [J]. *Acta Materialia*, 2006, 54(4): 953–961.
- [17] KUMAR V, FANG Z Z, FIFE P C. Phase field simulations of grain growth during sintering of two unequal-sized particles [J]. *Materials Science and Engineering A*, 2010, 528(1): 254–259.
- [18] ASP K, ÅGREN J. Phase-field simulation of sintering and related phenomena—A vacancy diffusion approach [J]. *Acta Materialia*, 2006, 54(5): 1241–1248.
- [19] KIM S G, KIM W T, SUZUKI T, ODE M. Phase-field modeling of eutectic solidification [J]. *Journal of Crystal Growth*, 2004, 261(1): 135–158.
- [20] SAUNDERS N. A review and thermodynamic assessment of the Al–Mg and Mg–Li systems [J]. *Calphad*, 1990, 14(1): 61–70.
- [21] PAN X M, LIN C, MORRAL J E, BRODY H D. An assessment of thermodynamic data for the liquid phase in the Al-rich corner of the Al–Cu–Si system and its application to the solidification of a 319 alloy [J]. *Journal of Phase Equilibria and Diffusion*, 2005, 26(3): 225–233.
- [22] HILLERT M. The compound energy formalism [J]. *Journal of Alloys and Compounds*, 2001, 320(2): 161–176.
- [23] FRIES S G, SUNDMAN B. Development of multicomponent thermodynamic databases for use in process modelling and simulations [J]. *Journal of Physics and Chemistry of Solids*, 2005, 66(2–4): 226–230.
- [24] LIU Y J, WANG J, DU Y, ZHANG L J, LIANG D. Mobilities and diffusivities in fcc Fe–X ( X=Ag, Au, Cu, Pd and Pt ) alloys [J]. *Calphad*, 2010, 34(3): 253–262.
- [25] ZINKEVICH M, MATTERN N, HANDSTEIN A, GUTFLEISCH O. Thermodynamics of Fe–Sm, Fe–H, and H–Sm systems and its application to the hydrogen–disproportionation–desorption–recombination (HDDR) process for the system Fe<sub>17</sub>Sm<sub>2</sub>–H<sub>2</sub> [J]. *Journal of Alloys and Compounds*, 2002, 339(1–2): 118–139.
- [26] HUANG W M, OPALKA S M, WANG D, FLANAGAN T B. Thermodynamic modelling of the Cu–Pd–H system [J]. *Calphad*, 2007, 31(3): 315–329.
- [27] MIETTINEN J. Thermodynamic description of the Cu–Fe–Zn system [J]. *Calphad*, 2008, 32(3): 514–519.
- [28] LOGINOVA I, ODQVIST J, AMBERG G, ÅGREN J. The phase-field approach and solute drag modeling of the transition to massive  $\gamma \rightarrow \alpha$  transformation in binary Fe–C alloys [J]. *Acta Materialia*, 2003, 51(5): 1327–1339.
- [29] VILLANUEVA W, GRÖNHAGEN K, AMBERG G, ÅGREN J. Multicomponent and multiphase simulation of liquid-phase sintering [J]. *Computational Materials Science*, 2009, 47(2): 512–520.
- [30] GUO Shi-ju. Theory of powders sintering [M]. Beijing: Metallurgical Industry Press, 2007: 15–25. (in Chinese)
- [31] HIRATA LOPEZ V M, HIRANO K. Ostwald ripening of  $\gamma$ -Fe precipitates in a Cu–1.5at% Fe alloy [J]. *Scripta Metallurgica et Materialia*, 1994, 31(2): 117–120.
- [32] BUFINGTON F S, HIRANO K, COHEN M. Self diffusion in iron [J]. *Acta Metallurgica*, 1961, 9(5): 434–439.
- [33] KUPER A, LETAW H, SLIFKIN J L, SONDKR E, TOMIZUKA C T. Self-diffusion in copper [J]. *Physical Review*, 1954, 96(5): 1224–1225.
- [34] SALJE G, FELLER-KNIEPMEIER M. The diffusion and solubility of iron in copper [J]. *Journal of Applied Physics*, 1978, 49(1): 229–232.
- [35] BRANDES E A, BROOK G B. *Smithells metals reference book* [M]. 7th ed. Woburn: Butterworth-Heinemann, 1992: 13.79–13.81.
- [36] ROTHMAN S J, PETERSON N L, WALTER C M, NOWICKI L J. The diffusion of copper in iron [J]. *Journal of Applied Physics*, 1968, 39(11): 5041–5044.
- [37] JAMES D W, LEAK G M. Grain boundary diffusion of iron, cobalt and nickel in alpha-iron and of iron in gamma-iron [J]. *Philosophical Magazine*, 1965, 12(117): 491–503.
- [38] BUTRYMOWICZ D B, MANNING J R, READ M E. Diffusion in copper and copper alloys [J]. *Journal of Physical and Chemical Reference Data*, 1976, 5(1): 103–200.

## 采用相场法研究多相粉末的烧结过程

张瑞杰<sup>1</sup>, 陈忠伟<sup>2</sup>, 方伟<sup>1</sup>, 曲选辉<sup>1,3</sup>

1. 北京科技大学 新材料技术研究院, 北京 100083;
2. 西北工业大学 凝固技术国家重点实验室, 西安 710072;
3. 北京科技大学 新金属材料国家重点实验室, 北京 100083

**摘要:** 针对多相粉末体系, 建立描述其烧结过程的相场模型。在该模型中, 界面由不同成分的各相混合组成, 通过热力学平衡确定界面中各相的成分; 除了体扩散之外, 也同时考虑了界面扩散和表面扩散。所建的模型被应用到 Fe-Cu 粉末的烧结过程。结果表明, 该模型能够定量地描述烧结过程中的微观组织演变以及溶质扩散等现象。

**关键词:** 相场模型; 烧结; 多相粉末; 热力学

(Edited by Hua YANG)